13th World Conference on Earthquake Engineering
Vancouver, B.C., Canada
August 1-6, 2004
Paper No. 2298

EFFECT OF SOIL-STRUCTURE INTERACTION AND SPATIAL VARIABILITY OF GROUND MOTION ON IRREGULAR BRIDGES: THE CASE OF THE KRYSTALLOPIGI BRIDGE

Anastasios SEXTOS[1], Andreas J. KAPPOS[2], Panayiotis MERGOS[3]

SUMMARY

This study focuses on the assessment of the curved, 638m long, twelve-span Krystallopigi bridge, which is currently under construction as part of the EGNATIA highway in northern Greece. An effort is made to investigate the potential influence of spatial variability of earthquake ground motion on curved bridges (as opposed to straight ones). It is shown that the structural performance of the particular curved bridge under earthquake loading is strongly affected by (a) the accuracy in modeling the properties of the incoming seismic wave field and the foundation subsoil and (b) the curvature and overall irregularity parameters.

INTRODUCTION

From all the parameters that define the non-linear dynamic response of complex structures like bridges, the input motion has by far the highest level of uncertainty. The last three decades, different approaches, methodologies and tools have been utilized to deal with this uncertainty and put it in a framework that can be quantified and thus uniformly interpreted by the practicing engineers and the scientific community. Along theses lines, the extensive use of refined response spectra worldwide is currently the primer tool for defining the input earthquake ground motion independently of the type of analysis that is to be used (i.e. equivalent static, response spectrum) while it is also used within the context of (spectrum compatible) accelerograms generation and time history analysis. Despite the fact that nowadays seismic design of important bridges is increasingly performed using dynamic analysis in the time domain, using natural or artificially generated earthquake records identical for all bridge supports, the question still arises whether such decision making process is still valid for extended structures. In particular for the case of bridges (especially long ones), it is clear that earthquake ground motion may significantly differ among the support points, in terms of amplitude, frequency content and arrival time, inducing under certain circumstances significant forces and deformations that would not develop if the assumption of synchronous excitation was adopted (Hao [1], Shinozuka & Deodatis [2], Zerva [3]). These spatial and temporal variations of seismic motion can be primarily attributed to four (a-d) factors (Der Kiureghian & Keshishian [4], Zerva [3]):

[1] Lecturer, Aristotle University of Thessaloniki
[2] Professor, Aristotle University of Thessaloniki
[3] Civil Engineer, MSc, Aristotle University of Thessaloniki

a) *Travelling of the waves* at a finite velocity, so that their arrival at each support point is out of phase

b) *Loss of coherency* in terms of statistical dependence, that is loss of signals 'similarity' due to multiple reflections, refractions and superpositioning of the incident seismic waves that occur during propagation

c) *Effect of local soil conditions* especially for cases that the soil profile through which motion propagates varies significantly. Local site conditions on the other hand have a much more complex effect than the spectral modification of the code design spectra. For multi-layer damped soil columns, both peak ground acceleration and frequency content at the surface motion are strongly dependent on soil and site conditions and the velocity contrast between the bedrock and the overlaying layers (Pitilakis [5])

d) *Attenuation of motion* due to geometrical spreading of the wave front and the loss of kinematic energy.

Additionally to the above, seismic motion is further modified by the foundation, depending on its relative flexibility with respect to the soil, since the foundation is not always able to vibrate according to the displacement field that is imposed to it by the incoming waves: As the bridge foundation is flexible, dissipates energy and interacts with the surrounding soil and the superstructure in such a way, that it filters seismic motion (kinematic interaction) while it is subjected to inertial forces generated by the vibration of the superstructure (inertial interaction). This phenomenon is very complex and its beneficial or detrimental effect on the dynamic response of the bridge is dependent on a series of parameters such as (Pender [6], Wolf [7], Gazetas & Mylonakis [8]) the intensity of ground motion, the dominant wavelengths, the angle of incidence of the seismic waves, the stromatography, the stiffness and damping of soil as well as the size, geometry, stiffness, slenderness and dynamic characteristics of the structure.

The nonuniform seismic excitation of bridges has been studied extensively by various researches that have established the fundamental framework to consider the potential role played by multiple support excitation, soil-structure interaction and/or the local soil conditions variation such as Zerva [3], Shinozuka et al. [9] and Simeonov et al. [10], among others. Nevertheless, the vast majority of the research performed focuses on cases of straight bridges, hence, the effect of asynchronous ground motion in the case of curved bridges and the sensitivity of the structure to the angle of incidence of the incoming wave field (Allam & Datta, [11], Ettouney et al. [12]), given its spatial variation, has not yet been studied in depth. The scope of this paper therefore, is to utilise the aforementioned experience that culminated into the development of a comprehensive approach (Sextos et al. [13]) to study the real case of a curved and long bridge structure and, thus, determine to what extent observations already made so far for straight bridges are valid in the case of significant curvature in plan.

OVERVIEW OF THE CASE STUDY

The Krystallopigi bridge is a twelve span structure of 638m total length (Fig. 1) that crosses a valley, as a part of the 680 km EGNATIA highway in northern Greece. The curvature radius is equal to 488m while its deck width is 13m. According to the initial design, the deck is a prestressed at its top flange concrete box girder section; concrete grade is B45 (characteristic cylinder strength f_{ck}=35 MPa) and prestressing steel grade 1570/1770 (f_y=1570 MPa). Piers are in reinforced concrete, concrete grade is B35 (f_{ck}=27.5MPa), steel grade Bst500s (f_y=500 MPa). For abutments and foundations B25 (f_{ck}=20 MPa) and Bst500s are used. The structure is supported on piers (M1-M11 in Fig. 2) of height that varies between 11 and 27m, For the end piers M1, M2, M3, M9, M10, M11 a bearing type pier-to-deck connection is adopted (see Fig. 3), while the interior piers are monolithically connected to the deck. It is noted that for practical reasons (i.e. anchorage of the prestressing cables) the initial 0.50x0.20m pier section is widened to 0.70x0.20m at the pier top range. The piers are supported on groups of piles of length and configuration that differs between support points due to the change of the soil profile along the bridge axis, an issue that has been accounted for in the calculation of the soil-foundation system properties.

Finite element analysis has been used for the assessment of the non-linear response of the bridge, involving the discretisation of the structure in 220 non-prismatic 3D beam elements (Fig. 4). For the piers connected to the deck through bearings, the movement along the longitudinal axis as well as the rotation around both the longitudinal and transverse axis is unrestrained. On the contrary, the existence of shear keys results to the prevention of transverse displacements and the movement and rotation along and about the vertical axis. For assessment purposes, alternative models with cracked concrete sections and flexible foundations were also studied and presented elsewhere (Mergos et al. [14]). The effective pier stiffness EI_{eff} was calculated from the initial slope of the moment-curvature relationship of the section at the location of the plastic hinge, as prescribed by Eurocode 8 (CEN, [15]) and the Greek Code (Ministry of Public Works [16]) for bridge design. The stiffness properties of the coupled soil-foundation pier, on the other hand, were calculated using the computer code ASING (Sextos et al. [13]).

A full design of the actual bridge (for usual, as well as seismic, actions) was carried out by the Greek consultancy firm DENCO (Athens). The seismic behavior of the designed bridge was assessed using non-linear static (pushover) analysis with the widely used F.E. program SAP2000 (Computers & Structures, 1999 [14]). For the definition of target displacements of the structure the response spectrum of the Greek Seismic Code (Ministry of Public Works [18]) was used. Soil conditions were taken to correspond to category 'B' of the Greek seismic code, which can be considered equivalent to subsoil class 'B' of Eurocode 8. For the considered Zone III of the Greek Code a peak ground acceleration of 0.24g was specified, while a behavior factor of 3.0 was adopted. The seismic design and assessment of the Krystallopigi bridge through non-linear static analysis indicates (Mergos et al. [14]) that the application of modern seismic codes resulted in a bridge able to resist earthquakes that exceeded the design level even by a factor of two. Displacement ductility factors of about 5 or more were estimated for both directions of the bridge and calculated overstrength varied from 35 to 70%.

Figure 1: Layout of the bridge configuration

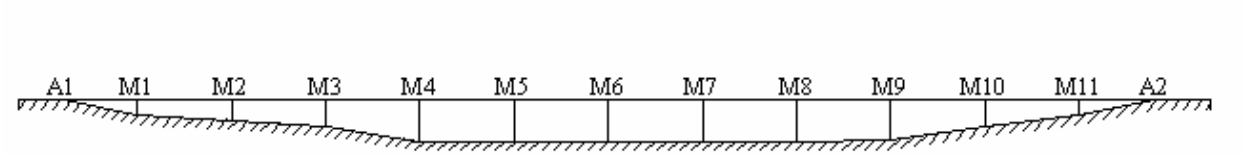

Figure 2: Overview of the Krystallopigi Bridge

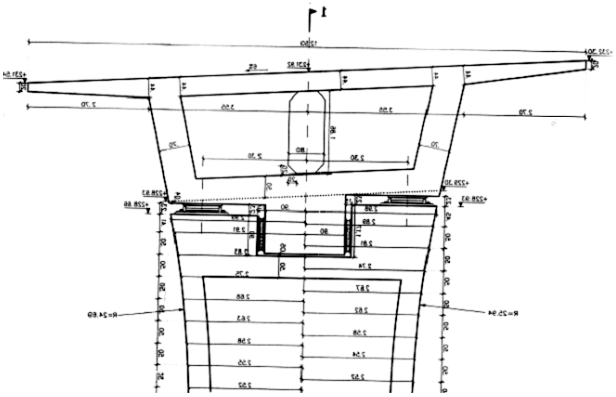

Figure 3: Non-monolithic pier-to-deck connection (end piers)

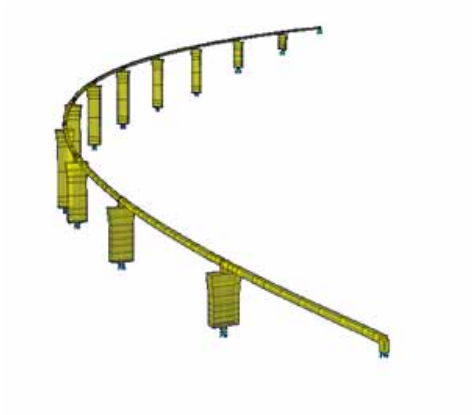

Figure 4: Layout of the 3D Finite element model

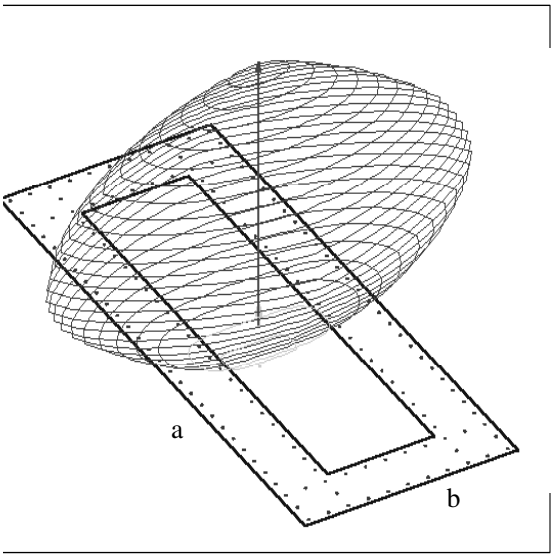

Figure 5: M-N interaction curves (in the 3D space) for the hollow piers

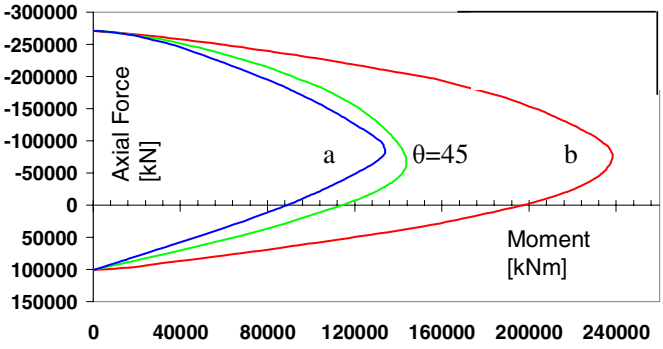

Figure 6: M-N interaction curves (in 2D space) along different axes of the pier

OVERVIEW OF THE APPLIED METHODOLOGY

Spatial Variability of Ground Motion

The coherency model of Luco and Wong [19] was selected among others to account for both the shear and the apparent wave velocity:

$$\gamma(\omega,\xi) = e^{-\left(\frac{\alpha\omega\xi}{V_s}\right)^2} \cdot e^{i\left(\frac{\alpha\omega\xi_L}{V_{app}}\right)} \tag{1}$$

the first term being an exponential decay of coherency with separation distance ξ and frequency ω, which decreases as soil becomes stiffer, while the second term represents the wave passage effect which produces longer signal arrival delay as the projected horizontal inter-station distance ξ and the frequency ω increase and the apparent velocity V_{app} decreases. With the simplifying assumption made of a common power spectrum for all support points, the n3n cross power spectral density matrix can then be written as:

$$[S(\omega)] = \begin{bmatrix} 1 & \gamma_{12}(i\omega,\xi) & ... & \gamma_{1n}(i\omega,\xi) \\ \gamma_{21}(i\omega,\xi) & 1 & ... & \gamma_{2n}(i\omega,\xi) \\ ... & ... & 1 & ... \\ \gamma_{n1}(i\omega,\xi) & \gamma_{n2}(i\omega,\xi) & ... & 1 \end{bmatrix} \cdot S_0(\bar{\omega}) \tag{2}$$

which is a Hermitian and positive definite matrix, that can be expressed as a product of a lower triangular matrix $[L(i\bar{\omega})]$ and its Hermitian matrix $[L(i\bar{\omega})]^H$:

$$[S(\omega)] = [L(i\bar{\omega})][L(i\bar{\omega})]^H \cdot S_0(\bar{\omega}) \tag{3}$$

where $\bar{\omega} = (2/3)\omega$ and $[L(i\bar{\omega})]$ is derived with the use of Choleski decomposition method as follows:

$$L(i\bar{\omega}) = \begin{bmatrix} l_{11}(\bar{\omega}) & 0 & .... & 0 \\ l_{21}(i\bar{\omega}) & l_{22}(\bar{\omega}) & .... & 0 \\ .... & .... & .... & .... \\ l_{n1}(i\bar{\omega}) & l_{n2}(i\bar{\omega}) & .... & l_{nn}(\bar{\omega}) \end{bmatrix} \tag{4}$$

Consequently, the distinct acceleration time histories at all points, that reflect the effect of time delay and loss of coherency only, can be expressed in the general form:

$$x_i(t) = 2\sum_{m=1}^{n}\sum_{l=1}^{N}\left|L_{jm}(\omega_{ml})\right|\sqrt{\Delta\omega}\cdot\cos[\omega_{ml}t + \theta_{jm}(\omega_{ml}) + \phi_{ml}] \tag{5}$$

where φ_{ml} are independent random phase angles, uniformly distributed in the range $(0,2\pi)$, N represents the Nyquist frequency $\bar{\omega}_N$, $\Delta\omega$ is the frequency step and θ_{jm} is the phase which is equal to:

$$\theta_{jm}(\bar{\omega}_{ml}) = \tan^{-1}\frac{\mathrm{Im}[l_{jm}(i\bar{\omega}_{ml})]}{\mathrm{Re}[l_{jm}(i\bar{\omega}_{ml})]} \tag{6}$$

The above uniform soil approach which accounts only for wave passage and loss of coherency and neglects the effect of local soil conditions has been used herein because it can provide ground motions that are reasonably uncorrelated, while, for the particular bridge under study, the soil conditions along its length where not significantly different. Moreover, potential coupling of the site response effect with the bridge curvature in plan would not assist towards the identification of the fundamental sensitivity of curved bridges to multiple support excitation.

ASYNCHRONOUS MOTION SCENARIOS

Within the context discussed above, the Krystallopigi bridge the partially correlated ground motions were generated using the computer code ASING (Sextos et al. [13]). A fixed duration of 20sec was selected since the problem is investigated in a relative sense, i.e. absolute response parameters are not of particular interest. Through the aforementioned code, zero final velocity and displacement was also achieved by applying baseline correction, while an iterative optimization procedure of updating the target power spectral density function was also performed.

Another important aspect is the investigation of the applicability of the above procedure for motions applied along different axes of the bridge, since this was a key issue in the present study. As a first simplification, the relative orientation of the wave propagation direction with respect to the orientation of the bridge can be accounted for by modifying the phase angle of the motion. Moreover, the spectral density function may be taken identical for both directions, based on the assumption that soil homogeneity and isotropy produce directionally independent site effects at least for vertically propagating S-waves, as typically assumed for engineering analysis purposes. The loss of coherency pattern is also assumed common in all directions. This simplifying assumption is in line with the vast majority of existing proposals but also because it has been verified through experimental observations (Hao, [1]), although later studies, e.g. Der Kiureghian & Keshishian [4]) consider coherency as path-dependent, hence direction-dependent. The recommended procedure is to assume, notwithstanding all the limitations discussed, that the use of the above procedure in all directions is valid, but carry out separate simulations, for various angles, in order to ensure that the corresponding motions will be fully uncorrelated.

To investigate the effects of geometric incoherence three sets (scenarios) of artificial records were used. In the first two, for two different target frequency spectra, the motion along support points is considered as fully correlated and the arrival delay is defined by the angle between the direction of seismic wave propagation with respect to the bridge axis and the soil properties that determine the shear wave propagation velocity. For the third case, both phase and amplitude vary in space. In particular:

(SCEN1) Actual Earthquake Motion recorded during the 1995 Kozani earthquake scaled to the target level of Peak Ground Acceleration (0.24g). Asynchronism pattern: Wave passage effect.

(SCEN2) Artificial Seismic Ground Motion compatible with the EC8 elastic response Spectrum scaled to the target level of Peak Ground Acceleration (0.24g). Asynchronism pattern: Wave passage effect (Figure 7)

(SCEN3) Artificial Seismic Ground Motion compatible with the EC8 elastic response Spectrum scaled at the target level of Peak Ground Acceleration (0.24g). Asynchornism pattern: Wave passage and loss of coherency effect (Figures 8, 9)

Depending on the direction of excitation with respect to the bridge axis, all three sets of motions are generated within the following parametric analysis scheme:

- Uniform ground motion (displacement excitation)
- Asynchronous motion (arriving at velocity Vs=400m/sec along the bridge chord axis)
- Asynchronous motion (arriving at velocity Vs=400m/sec at an angle of 30^o to the bridge chord axis)
- Asynchronous motion (arriving at velocity Vs=400m/sec at an angle of 45^o to the bridge chord axis)
- Asynchronous motion (arriving at velocity Vs=400m/sec at an angle of 60^o to the bridge chord axis)
- Asynchronous motion (arriving at velocity Vs=400m/sec at an angle of 75^o to the bridge chord axis)
- Asynchronous motion (arriving at velocity Vs=400m/sec at an angle of 90^o to the bridge chord axis)

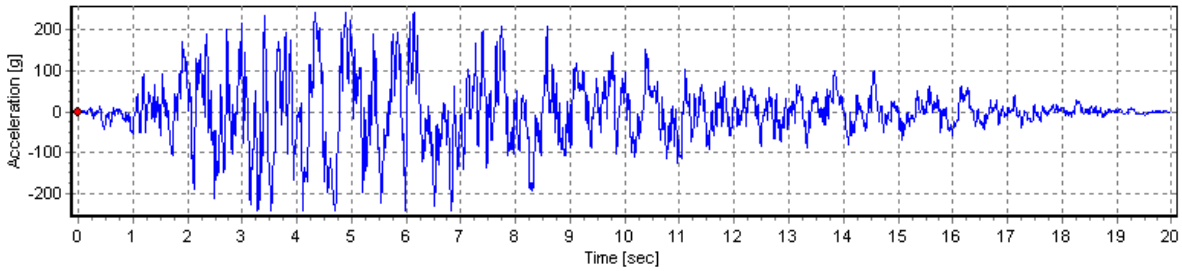

Figure 7: Artificial earthquake ground motion generated to match the Eurocode 8 spectrum

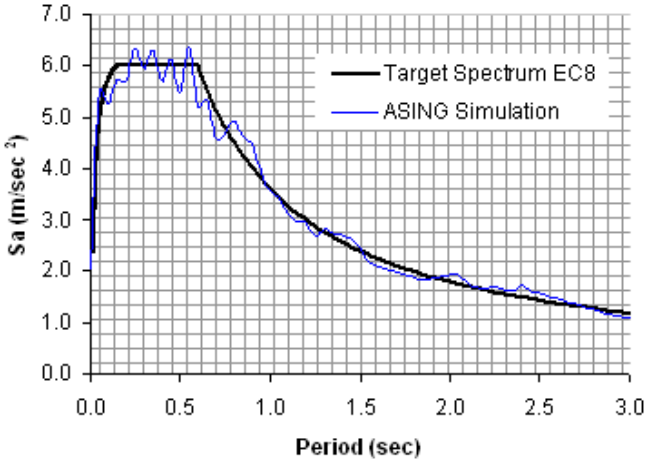

Figure 8: Comparison between the mean response spectrum of the artificially generated earthquake ground motion and the target Eurocode 8 Spectrum

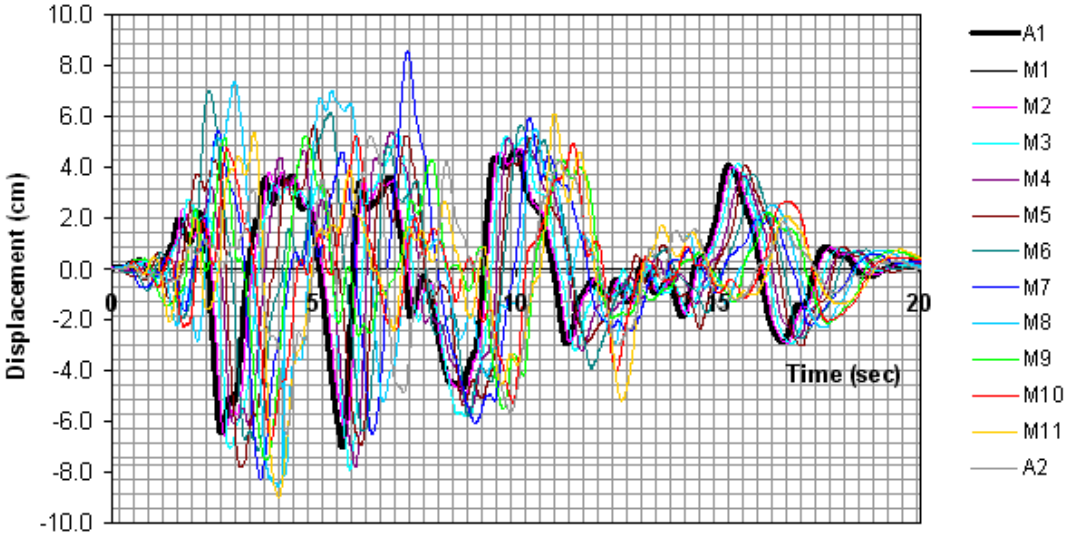

Figure 9: Simulated earthquake ground motions displacement time histories for all bridge support that match the Eurocode 8 spectrum and account for the wave passage and loss of coherency effects

Wave Passage Effect $d_{asyncrounous} / d_{synchronous}$

Response along the x-x axis

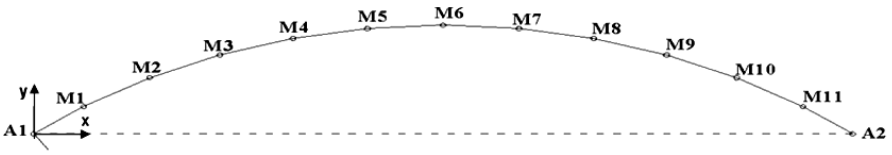

propagation direction	motion													
0° - parallel to chord	synchronous	1.00	1.00	1.00	1.00	1.00	1.00	1.00	1.00	1.00	1.00	1.00	1.00	1.00
0^0 - parallel to chord	wave passage	0.94	0.95	0.95	0.95	0.97	0.98	0.94	0.95	0.97	0.97	0.97	0.97	0.98
30°	wave passage	0.97	0.97	0.98	0.97	0.95	0.94	0.94	0.95	0.98	0.97	0.95	0.94	0.93
45°	wave passage	0.98	0.99	0.98	0.98	0.97	0.96	0.96	0.97	0.99	0.99	0.97	0.95	0.95
60°	wave passage	0.99	0.99	0.99	0.99	0.99	0.99	0.98	0.99	1.01	1.01	0.99	0.97	0.97
75°	wave passage	1.00	0.99	0.99	1.00	1.00	0.99	0.99	1.00	1.01	1.01	0.99	0.98	0.98
90° -perpendicular to chord	wave passage	0.99	0.99	0.99	1.00	1.00	1.00	1.00	1.00	1.00	1.00	0.99	0.99	0.99

Response along the y-y axis

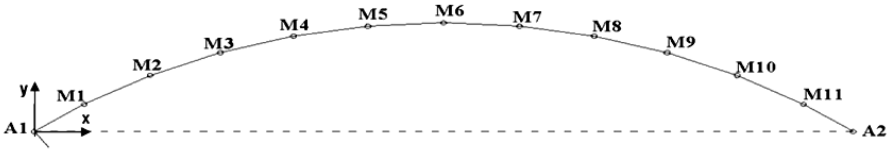

propagation direction	motion													
0° - parallel to chord	synchronous	1.00	1.00	1.00	1.00	1.00	1.00	1.00	1.00	1.00	1.00	1.00	1.00	1.00
0^0 - parallel to chord	wave passage	0.81	0.90	0.89	0.74	0.95	0.69	**1.95**	0.84	0.87	1.04	0.93	0.73	0.99
30°	wave passage	0.78	0.90	0.88	0.99	**1.16**	0.74	**1.99**	0.81	0.87	0.93	1.03	0.83	**1.10**
45°	wave passage	0.80	0.88	0.83	1.02	**1.15**	0.78	**1.93**	0.77	0.96	0.92	**1.07**	0.80	**1.11**
60°	wave passage	0.73	0.76	0.92	0.88	**1.17**	0.90	**1.43**	0.72	1.03	0.99	1.03	0.81	1.02
75°	wave passage	0.87	0.87	0.98	0.91	**1.14**	0.97	**1.33**	0.84	1.04	1.02	1.03	0.92	1.00
90° -perpendicular to chord	wave passage	0.94	0.90	0.97	1.04	0.99	1.04	1.04	1.01	0.97	0.99	0.91	1.00	0.90

Figure 10: Ratio of the multiply supported over synchronously excited bridge displacements (SCEN1)

Wave Passage Effect $M_{asyncrounous} / M_{synchronous}$

Response along the x-x axis

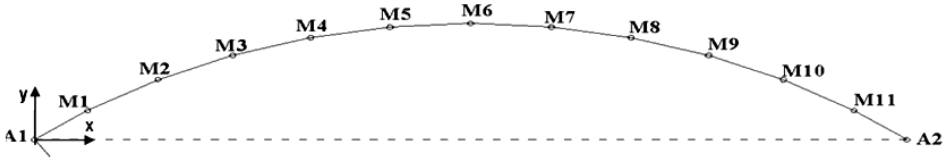

propagation direction	motion												
0° - parallel to chord	synchronous	1.00	1.00	1.00	1.00	1.00	1.00	1.00	1.00	1.00	1.00	1.00	
0^0 - parallel to chord	wave passage	0.93	0.97	1.04	0.91	0.93	0.93	0.94	0.97	1.02	0.98	0.94	
30°	wave passage	0.93	0.97	1.04	0.93	0.95	0.95	0.96	0.99	1.02	0.97	0.94	
45°	wave passage	0.94	0.97	1.03	0.95	0.96	0.96	0.98	1.00	1.02	0.97	0.92	
60°	wave passage	0.96	0.99	1.01	0.98	0.97	0.98	0.99	1.00	1.02	0.98	1.05	
75°	wave passage	0.98	0.99	1.00	1.00	0.98	0.98	1.00	1.00	1.06	0.99	1.02	
90° -perpendicular to chord	wave passage	1.00	1.00	1.00	1.00	0.99	0.99	0.99	0.99	0.99	1.00	0.96	

Response along the y-y axis

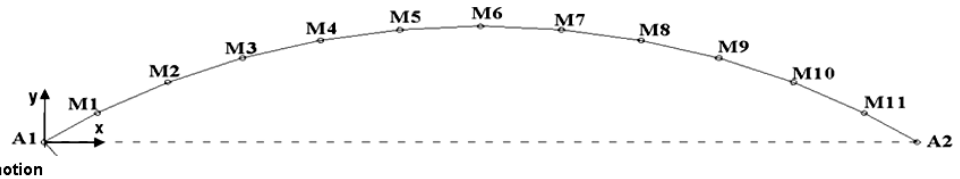

propagation direction	motion												
0° - parallel to chord	synchronous	1.00	1.00	1.00	1.00	1.00	1.00	1.00	1.00	1.00	1.00	1.00	
0^0 - parallel to chord	wave passage	1.00	1.07	1.02	**1.18**	0.70	**2.02**	0.88	0.76	**1.12**	0.88	1.01	
30°	wave passage	1.01	1.04	1.09	**1.20**	0.72	**2.05**	0.84	0.86	**1.13**	0.86	1.08	
45°	wave passage	1.07	0.98	**1.12**	**1.18**	0.77	**1.99**	0.78	0.96	**1.10**	0.80	1.09	
60°	wave passage	1.06	1.05	0.96	**1.19**	0.88	**1.47**	0.74	1.04	0.97	0.81	1.06	
75°	wave passage	0.82	1.07	0.97	**1.16**	0.97	**1.34**	0.86	1.04	0.96	0.94	1.03	
90° -perpendicular to chord	wave passage	0.90	1.07	1.09	0.99	1.04	1.05	1.04	0.98	1.01	1.03	0.94	

Figure 11: Ratio of the asynchronously over synchronously excited bridge pier base bending moments (SCEN1)

Wave passage effect

For an in-depth study of the problem, it is important to establish a parametric analysis scheme that allows assessing the influence of each particular parameter separately. Along these lines, it is decided to focus on the relative response (i.e. pier top absolute displacements and pier base bending moments) of the asynchronously excited structure with respect to the synchronous excitation case. Clearly, a value of the response ratio that exceeds 1.0 represents the unfavourable case of displacement or bending moment increase, while beneficial effect, i.e. reduction in the action effect, corresponds to a ratio less than 1.0. It is also recalled that the response parameters refer to both the transverse (i.e. y-y, perpendicular to the chord) and longitudinal (x-x, parallel to the chord) direction.

According to SCEN1, the bridge is subjected to an artificial ground motion whose frequency content is compatible with the 1995 Kozani earthquake, scaled to a peak ground acceleration of 0.24g and propagating as a fully correlated wave field that travels at a constant velocity but at different angles with respect to the bridge chord axis (x-x). Figure 10 illustrates that accounting for the aforementioned wave travel leads, independently of the angle of incidence employed, to uniformly decreased (by 5-10%), with respect to the commonly used synchronous excitation, displacements along the x-x axis, and substantially decreased (up to 30%) displacements along the perpendicular axis (y-y). Nevertheless, in the latter direction, few but extreme cases are observed where the displacements of the middle piers M4 and M6 are almost doubled despite the reduction observed for their neighboring (M5, M7, M8) piers. The same trend can also be seen when assessing the pier base bending moments (Figure 11). This trend, which has not been observed in previous extensive parametric analyses of 20 straight bridges (Sextos et al.[21]), may be possibly attributed to the bridge irregularity (i.e. curvature in plan and bearing type pier-deck connections at some piers only) and the subsequent complex dynamic behaviour that is more sensitive to potential higher mode excitation, that numerous analyses (Dumanoglou & Soyluk [22], Ettouney et al. [12], Sextos et al. [21]) have shown that asynchronous motion triggers. However, it is difficult to generalize the observations made above because the structural configuration, which is constant in this study, strongly influences both the bridge's dynamic response and its sensitivity to multiple support excitation.

Effect of ground motion angle

Given the curvature in plan of the Kristallopigi bridge as well as the aforementioned simulation strategy to represent the arrival delay of the incoming waves, it is of particular interest to attempt to isolate the importance of the angle between the direction of excitation and the longitudinal (chord) axis of the bridge. Figure 12 presents the displacements of the deck at the locations of the pier top for cases of multiple support excitation at different angles normalized to the reference case where waves travel parallel to the bridge chord. It is shown, that in most cases, the maximum displacement response does not occur for zero angle of incidence (i.e. propagation parallel to the bridge chord), an observation that has also been made by other researchers (Allam & Datta [11]). Moreover, the degree of displacement modification along the x-x (chord) axis is rather small (i.e. it does not vary by more than 8%) independently of the angle, leading to the conclusion that, in terms of displacements perpendicular to the chord and for fully correlated motions that arrive at a particular time shift at various support points, it is far more important to consider the *time* of incidence at the piers rather than the *angle* of incidence.

On the contrary, the rotation of the wavefront plane at various angles strongly affects the maximum dynamic displacements along the y-y axis, as seen in Figure 12. Of course, this is indeed anticipated and especially in the extreme case of 90^o angle, which is essentially the case of excitation along the y-y direction, the response of the structure along this direction should have been maximized. Nevertheless, it is observed that on average the increase of the maximum pier top displacements is not proportional to the increase of the angle of incidence. In other words, asynchronous excitation at an angle of 30^o compared to

90°, may result to a higher increase of the displacements of piers M4, M6, M10 and abutment A2 with respect to the displacements that would have been observed for wave propagation parallel to the chord.

Effect of input motion characteristics

As seismic waves are not fully correlated and their frequency content does not necessarily match that of the Kozani earthquake, it is deemed very important to investigate the relative response of the bridge for cases that the characteristics of the earthquake ground motion are different (as a first level of modification, the target Eurocode 8 Spectrum is used – SCEN2). Repeating the aforementioned parametric analysis scheme by generating fully coherent motions that match the Eurocode 8 spectrum (Figure 9) it is seen (Figures 13 and 14) that the same trends (albeit to a relatively lower degree) presented above are also observed. As a result, it is of particular interest to study the effect of input motion characteristics in the light of partial statistical dependence as described in the SCEN3 case that follows.

Effect of wave coherency loss

Within the framework of the more refined approach (SCEN3), the motions generated at all support points show the required degree of uncorrelation, as described by equation 1. A sample accelerogram, that has also been used as the unique waveform in the previous case is shown in Figure 7, while the complete set of input displacement time histories that on average matched the EC8 target spectrum (Figure 8) is illustrated in Figure 9.

Wave Passage Effect $d_{\text{asyncrounous various angles}} / d_{\text{asynchronous // chord}}$

Response along the x-x axis

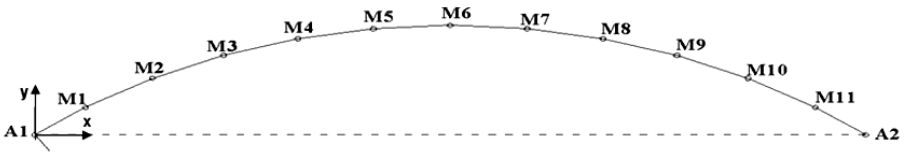

propagation direction	motion													
0° - parallel to chord	wave passage	1.00	1.00	1.00	1.00	1.00	1.00	1.00	1.00	1.00	1.00	1.00	1.00	1.00
30°	wave passage	1.03	1.02	1.03	1.02	0.98	0.96	1.00	1.00	1.01	1.00	0.98	0.96	0.95
45°	wave passage	1.05	1.04	1.04	1.03	1.00	0.98	1.02	1.02	1.02	1.02	0.99	0.98	0.96
60°	wave passage	1.05	1.04	1.04	1.04	1.02	1.01	1.05	1.05	1.04	1.04	1.02	1.00	0.99
75°	wave passage	1.06	1.05	1.04	1.05	1.03	1.02	1.05	1.05	1.04	1.04	1.02	1.01	1.00
90° -perpendicular to chord	wave passage	1.05	1.04	1.04	1.05	1.03	1.02	1.06	1.05	1.03	1.03	1.02	1.02	1.01

Response along the y-y axis

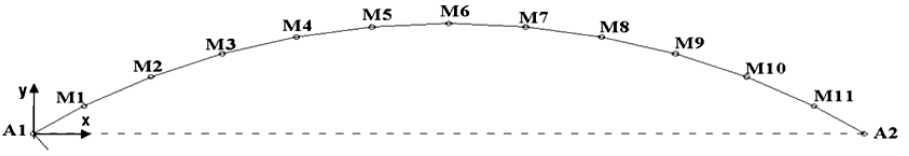

propagation direction	motion													
0° - parallel to chord	wave passage	1.00	1.00	1.00	1.00	1.00	1.00	1.00	1.00	1.00	1.00	1.00	1.00	1.00
30°	wave passage	0.97	1.00	0.99	**1.34**	**1.23**	1.07	1.02	0.97	0.99	0.89	1.10	1.13	1.11
45°	wave passage	0.99	0.97	0.93	**1.38**	**1.21**	1.13	0.99	0.91	1.10	0.88	1.15	1.09	1.13
60°	wave passage	0.91	0.84	1.03	**1.18**	**1.23**	**1.30**	0.74	0.86	**1.19**	0.95	1.10	1.11	1.03
75°	wave passage	1.07	0.97	1.10	**1.22**	**1.20**	**1.41**	0.68	1.00	**1.19**	0.98	1.10	**1.26**	1.01
90° -perpendicular to chord	wave passage	**1.16**	1.00	1.09	**1.40**	1.05	**1.51**	0.53	**1.20**	1.12	0.95	0.97	**1.38**	0.91

Figure 12: Effect of angle of excitation on the extent of the bridge displacement modification due to multiply support excitation (SCEN1)

Wave Passage Effect $d_{asyncrounous} / d_{synchronous}$

Response along the x-x axis

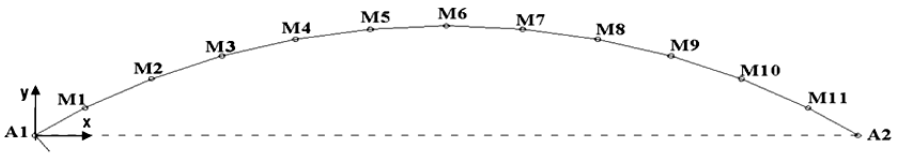

propagation direction	motion													
0° - parallel to chord	synchronous	1.00	1.00	1.00	1.00	1.00	1.00	1.00	1.00	1.00	1.00	1.00	1.00	1.00
0° - parallel to chord	wave passage	0.94	0.94	0.94	0.95	0.96	0.96	0.96	0.95	0.95	0.95	0.95	0.95	0.95
30°	wave passage	0.96	0.96	0.96	0.97	0.98	0.98	0.97	0.97	0.97	0.97	0.97	0.97	0.97
45°	wave passage	0.98	0.97	0.98	0.98	0.99	0.99	0.98	0.98	0.98	0.98	0.98	0.98	0.98
60°	wave passage	0.99	0.99	0.99	0.99	1.00	0.99	0.99	0.99	0.99	0.99	0.99	0.99	0.99
75°	wave passage	0.99	0.99	1.00	1.00	1.00	1.00	0.99	0.99	1.00	1.00	1.00	1.00	1.00
90° -perpendicular to chord	wave passage	1.00	1.00	1.00	1.00	1.00	0.99	0.99	0.99	0.99	1.00	1.00	1.00	1.00

Response along the y-y axis

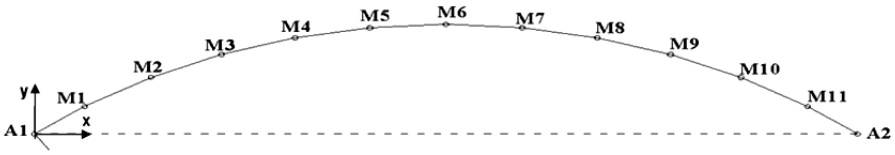

propagation direction	motion													
0° - parallel to chord	synchronous	1.00	1.00	1.00	1.00	1.00	1.00	1.00	1.00	1.00	1.00	1.00	1.00	1.00
0° - parallel to chord	wave passage	0.82	0.97	0.98	0.95	0.71	0.63	**1.28**	0.95	0.81	0.83	1.01	0.93	0.85
30°	wave passage	0.86	1.05	0.99	0.96	0.81	0.70	**1.34**	0.94	0.84	0.88	0.98	0.92	0.89
45°	wave passage	0.95	1.11	1.02	0.93	0.91	0.78	**1.43**	0.90	0.86	0.92	1.01	0.96	0.91
60°	wave passage	0.94	1.04	1.02	0.97	1.04	0.94	**1.34**	0.77	0.91	0.99	1.03	0.97	0.96
75°	wave passage	0.94	1.02	0.97	1.02	1.03	0.99	**1.27**	0.79	0.94	1.00	1.00	0.97	1.00
90° -perpendicular to chord	wave passage	0.99	1.03	0.95	1.02	0.98	1.02	0.97	0.96	0.99	0.99	0.97	0.98	1.05

Figure 13: Ratio of the multiply supported over synchronously excited bridge displacements (SCEN2)

Wave Passage Effect $M_{asyncrounous} / M_{synchronous}$

Response along the x-x axis

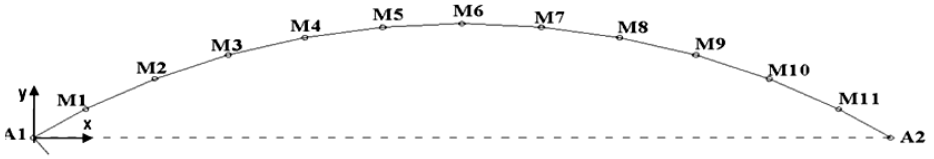

propagation direction	motion											
0° - parallel to chord	synchronous	1.00	1.00	1.00	1.00	1.00	1.00	1.00	1.00	1.00	1.00	1.00
0° - parallel to chord	wave passage	0.97	0.98	1.01	0.95	0.96	0.96	0.95	0.95	1.07	0.98	0.96
30°	wave passage	0.97	0.98	1.01	0.97	0.98	0.97	0.97	0.97	1.09	0.98	0.97
45°	wave passage	0.97	0.99	1.01	0.98	0.99	0.98	0.98	0.98	1.12	0.97	0.98
60°	wave passage	0.98	0.99	1.00	1.00	0.99	0.99	0.99	0.99	1.06	0.99	0.99
75°	wave passage	0.99	0.99	1.00	1.00	1.00	0.99	0.99	0.99	1.04	0.99	1.00
90° -perpendicular to chord	wave passage	0.99	1.00	1.00	1.00	0.99	0.99	0.99	0.99	1.01	1.00	0.99

Response along the y-y axis

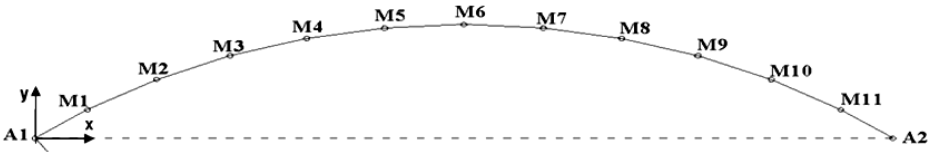

propagation direction	motion											
0° - parallel to chord	synchronous	1.00	1.00	1.00	1.00	1.00	1.00	1.00	1.00	1.00	1.00	1.00
0° - parallel to chord	wave passage	**1.23**	1.03	0.98	0.70	0.64	**1.25**	0.90	0.81	0.86	1.14	0.93
30°	wave passage	**1.20**	1.08	0.99	0.81	0.69	**1.33**	0.85	0.84	0.95	1.14	0.96
45°	wave passage	**1.24**	1.10	0.94	0.92	0.77	**1.43**	0.81	0.86	0.96	**1.21**	0.97
60°	wave passage	1.08	1.10	1.08	1.05	0.94	**1.33**	0.77	0.91	0.98	1.11	0.98
75°	wave passage	1.03	0.95	**1.11**	1.04	0.99	**1.26**	0.80	0.94	0.97	1.17	1.00
90° -perpendicular to chord	wave passage	1.04	1.00	1.07	0.98	1.02	0.97	0.96	0.99	0.94	1.15	1.00

Figure 14: Ratio of the asynchronously over synchronously excited bridge pier base bending moments (SCEN2)

Wave Passage Effect $d_{asyncrounous} / d_{synchronous}$

Response along the x-x axis

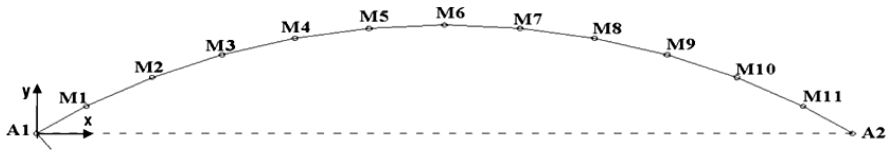

propagation direction	motion													
0° - parallel to chord	synchronous	1.00	1.00	1.00	1.00	1.00	1.00	1.00	1.00	1.00	1.00	1.00	1.00	1.00
0^0 - parallel to chord	θ+γ(ω)	0.78	0.77	0.77	0.77	0.76	0.76	0.76	0.76	0.76	0.75	0.76	0.76	0.76
30°	θ+γ(ω)	0.78	0.77	0.77	0.77	0.76	0.76	0.76	0.76	0.76	0.75	0.76	0.76	0.76
45°	θ+γ(ω)	0.54	0.54	0.54	0.54	0.54	0.54	0.54	0.54	0.54	0.53	0.53	0.53	0.53
60°	θ+γ(ω)	0.78	0.77	0.77	0.77	0.76	0.76	0.76	0.76	0.76	0.75	0.76	0.76	0.76
75°	θ+γ(ω)	0.95	0.94	0.93	0.93	0.92	0.92	0.91	0.91	0.92	0.92	0.92	0.92	0.93
90° -perpendicular to chord	θ+γ(ω)	0.77	0.77	0.76	0.76	0.76	0.75	0.75	0.75	0.75	0.75	0.75	0.75	0.76

Response along the y-y axis

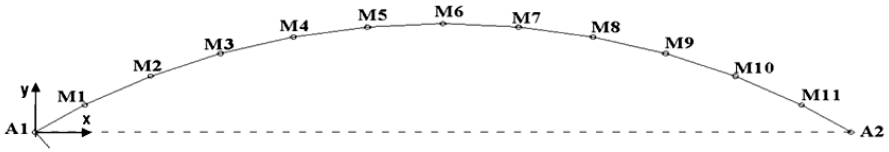

propagation direction	motion													
0° - parallel to chord	synchronous	1.00	1.00	1.00	1.00	1.00	1.00	1.00	1.00	1.00	1.00	1.00	1.00	1.00
0^0 - parallel to chord	θ+γ(ω)	0.93	1.11	1.03	0.77	0.54	0.33	0.80	0.58	0.50	0.66	1.00	0.77	0.80
30°	θ+γ(ω)	0.93	1.11	1.03	0.77	0.54	0.33	0.80	0.58	0.50	0.66	1.00	0.77	0.80
45°	θ+γ(ω)	0.94	1.09	0.99	0.66	0.40	0.27	0.71	0.59	0.37	0.53	1.01	0.62	0.77
60°	θ+γ(ω)	0.93	1.11	1.03	0.77	0.54	0.33	0.80	0.58	0.50	0.66	1.00	0.77	0.80
75°	θ+γ(ω)	0.94	1.15	1.08	0.84	0.62	0.36	0.78	0.73	0.65	0.77	1.00	0.89	0.85
90° -perpendicular to chord	θ+γ(ω)	0.94	1.07	1.00	0.77	0.53	0.34	0.77	0.59	0.51	0.64	0.98	0.61	0.74

Figure 15: Ratio of the multiply supported over synchronously excited bridge displacements (SCEN3)

Wave Passage Effect $M_{asyncrounous} / M_{synchronous}$

Response along the x-x axis

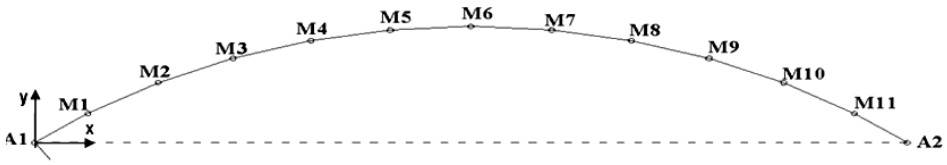

propagation direction	motion												
0° - parallel to chord	synchronous	1.00	1.00	1.00	1.00	1.00	1.00	1.00	1.00	1.00	1.00	1.00	
0^0 - parallel to chord	θ+γ(ω)	0.92	0.91	1.18	0.76	0.77	0.77	0.75	0.77	1.00	0.92	0.79	
30°	θ+γ(ω)	0.92	0.91	1.18	0.76	0.77	0.77	0.75	0.77	1.00	0.92	0.79	
45°	θ+γ(ω)	0.93	0.91	1.16	0.53	0.55	0.57	0.55	0.55	1.00	0.92	0.71	
60°	θ+γ(ω)	0.92	0.91	1.18	0.76	0.77	0.77	0.75	0.77	1.00	0.92	0.79	
75°	θ+γ(ω)	0.92	0.92	1.17	0.92	0.92	0.91	0.91	0.93	0.99	0.92	0.82	
90° -perpendicular to chord	θ+γ(ω)	0.92	0.92	1.17	0.75	0.76	0.76	0.75	0.76	0.99	0.93	0.60	

Response along the y-y axis

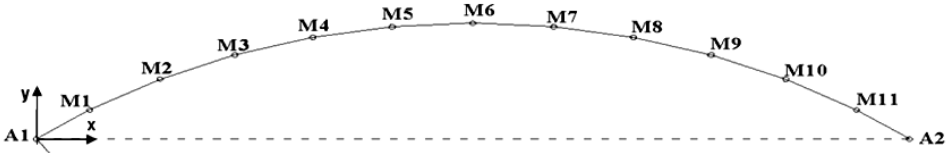

propagation direction	motion												
0° - parallel to chord	synchronous	1.00	1.00	1.00	1.00	1.00	1.00	1.00	1.00	1.00	1.00	1.00	
0^0 - parallel to chord	θ+γ(ω)	**1.32**	1.16	0.92	0.56	0.33	0.77	0.57	0.48	0.71	**1.67**	0.78	
30°	θ+γ(ω)	**1.32**	1.16	0.92	0.56	0.33	0.77	0.57	0.48	0.71	**1.67**	0.78	
45°	θ+γ(ω)	**1.27**	1.09	0.77	0.39	0.29	0.68	0.58	0.35	0.73	**1.64**	0.61	
60°	θ+γ(ω)	**1.32**	1.16	0.92	0.56	0.33	0.77	0.57	0.48	0.71	**1.67**	0.78	
75°	θ+γ(ω)	**1.38**	**1.21**	0.99	0.63	0.38	0.76	0.71	0.64	0.67	**1.62**	0.87	
90° -perpendicular to chord	θ+γ(ω)	**1.25**	1.15	0.91	0.55	0.35	0.78	0.58	0.55	0.78	**2.24**	0.77	

Figure 16: Ratio of the asynchronously over synchronously excited bridge pier base bending moments (SCEN3)

When the Kristallopigi bridge is subjected to the aforementioned set of motions, the overall dynamic response of the structure is significantly affected as compared to the commonly used (reference) synchronous excitation case. In particular, Figure 15 shows a substantial and rather global reduction (that reaches 70% in extreme cases) of displacements parallel to the chord (x-x) that with few exceptions is also observed for the perpendicular direction. This reduction in the absolute displacements that is attributed to the lack of correlation in the motion of the support points has also been observed in other studies (i.e. Tubino et al. [23] , Sextos et al. [21]).

It is also notable that although the increase in the variability of the input leads to an increase in pier top response variability (i.e. the range of pier maxima is wider), the latter can by no means be considered proportional to the first. In other words, significantly less coherent motions do not necessarily imply proportionally varying pier response, rendering the absolute displacement modification rather unpredictable.

In terms of pier base bending moments, it is seen that, especially, along the y-y (i.e perpendicular to the bridge chord) axis, the forces developed are substantially affected by the spatially variable character of motion (a reduction of up to 70% is observed together with an increase that exceeds 100%). As a result, it is clear that asynchronous motion cannot easily be replaced by an alternative 'reference' uniform motion (Zanardo et al. [24], Sextos et al. [21]). Nevertheless, this trend seems rather independent of the angle of incidence, verifying the observation made, that the particular curved bridge is far more sensitive to the spatially variable nature of ground motion than to the direction of wave propagation. Such a strong sensitivity of the bridge to the characteristics of asynchronous motion highlight that the value of 600m length suggested by EC8 provisions as the threshold for starting to consider asynchronous excitation effects, appears to need to be lowered in the case of curved bridges.

CONCLUSIONS

This study addresses the problem of asynchronous motion in curved bridges by studying the dynamic response of the 638m long, twelve-span, irregular in plan and height Krystallopigi bridge under multiple support excitation. Three different scenarios of spatially variable input have been used, compatible with real motions and the Eurocode 8 spectrum, leading to a set of parametric analyses.

The conclusions drawn can be summarised as follows:

- There is a significant difficulty to predict the effect of wave arrival delay and loss of coherency in the case of curved bridges since both pier base bending moments and pier top absolute displacements tend to decrease or increase by a factor of two for specific cases.
- Given all the limitations imposed by this inevitably case-dependent study, there is a observed tendency that when the particular bridge is multiply excited through a more refined simulation process that allows the generation of partially uncorrelated motions, its response in terms of displacements is generally beneficial, but significant pseudo-dynamic forces that develop lead to a significant increase in stresses locally.
- In the light of asynchronous motion, the angle of incidence of the incoming spatially variable waves seems to play a secondary role in the overall dynamic response of the studied bridge.

ACKNOWLEDGEMENT

The writers would like to thank EGNATIA ODOS S.A. for providing all available data and information with respect to the design of the Krystallopigi bridge.

REFERENCES

1. Hao H. (1989) Effects of spatial variation of ground motions on large multiply-supported structures. UBC/EERC-89/06, Berkeley: EERC, University of California, 1989.
2. Shinozuka M, Deodatis G. Effect of Spatial Variation of Earthquake Ground Motion on Seismic Response of Bridges. Proc. of the FHWA/NCEER Workshop on the National Representation of Seismic Motion, Tech. Rept, 97-0010; National Center for Earthquake Engineering Research , Buffalo, N.Y, 1997: 343-358.
3. Zerva A. Spatial Variability of Seismic Motions Recorded Over Extended Ground Surface Areas, in Wave Motion in Earthquake Engineering, Volume in the Series Advances in Earthquake Engineering, Editors: E. Kausel and G.D. Manolis, WIT Press, 1999.
4. Der Kiureghian A, Keshishian P. Effects of incoherence, wave passage and spatially varying site conditions on bridge response. Proceedings of the FHWA/NCEER Workshop on the National Representation of Seismic Motion, Tech. Rept, 97-0010; National Center for Earthquake Engineering Research , Buffalo, N.Y, 1997: 393-407.
5. Pitilakis K. "Chapter 5: Site effects". In: "Recent Advances in Earthquake Geotechnical Engineering & Microzonation" (A. Ansal, ed.), Kluwer Publications, 2004.
6. Pender MJ. Aseismic pile foundation design analysis, Bulletin of the New Zealand National Society on Earthquake Engineering 1993; 26(1): 49-161.
7. Wolf, JP. Foundation vibration analysis using simple physical models; Prentice Hall, 1994.
8. Gazetas G, & Mylonakis G. Seismic soil-structure interaction: new evidence and emerging issues, Geotechnical Special Publication 75, Geotechnical Earthquake Engineering and Soil Dynamics III, American Society of Civil Engineers, Reston, Virginia, **2** ; 1998: 1119-1174.
9. Shinozuka M, Saxena V, Deodatis, G. Effect of Spatial Variation of Ground Motion on Highway Structures, MCEER-00-0013, Multidisciplinary Center for Earthquake Engineering Research, Buffalo, N.Y., 2000.
10. Simeonov V, Mylonakis G, Reinhorn A, Buckle, I. Implications of spatial variation of ground motion on the seismic response of bridges: Case study, Proceedings of the FHWA/NCEER Workshop on the National Representation of Seismic Motion, Tech. Rept, 97-0010; National Center for Earthquake Engineering Research , Buffalo, N.Y, 1997: 359-392.
11. Allam, S. & Datta, T. "Seismic response of a cable-stayed bridge deck under multi-component non-stationary random ground motion:, Earthquake Engineering and Structural Dynamics, Vol. 33, 2004: 375-393.
12. Ettouney, M., Hapij, A. and Gajer, R "Frequency-domain analysis of long span bridges subjected to non-uniform seismic motions', Journal of Bridge Engineering, ASCE, Vol. 6, No. 6, 2001: 577-586.
13. Sextos, A., Pitilakis, K. and Kappos, A. "A global approach for dealing with spatial variability, site effects and soil-structure-interaction for non-linear bridges: a. verification study", Earthquake Engineering and Structural Dynamics, Vol. 4, 2003: 607-629.
14. Mergos, P., Sextos, A and Kappos, A. 'Seismic assessment of a major bridge using pushover analysis', International Conference on Computational & Experimental Engineering and Sciences, CD-ROM Vol. , paper no. 333, Corfu July, 2003.
15. CEN. Eurocode 8 "Design provisions for earthquake resistance of structures. Part 2: Bridges", ENV 1998-2, CEN, Brussels, 1994.
16. Ministry of Public Works "Guidelines for Seismic Design of Bridges", E39/99, Athens, 1999
17. Computers and Structures Inc. "SAP2000: Three dimensional static and dynamic finite element analysis and design of structures", Berkeley, California, 1999.
18. Ministry of Public Works "Greek Seismic Code (E.A.K. 2000)", Athens, 2000.
19. Luco JE, Wong HL. "Response of a rigid foundation to a spatially random ground motion", Earthquake Engineering and Structural Dynamics Vol. 14, 1986: 891-908.

20. Deodatis G. “Simulation of ergodic multi-variate stochastic processes”, Journal of Engineering Mechanics, Vol 128(8), 1996: 778-787.
21. Sextos, A. ; Pitilakis, K and A. Kappos “Inelastic dynamic analysis of RC bridges accounting for spatial variability of ground motion, site effects and soil-structure interaction phenomena. Part 2: Parametric Analysis”, Earthquake Engineering and Structural Dynamics, Vol. 32(4), 2003: 629-652.
22. Dumanoglou, A. & Soyluk, K. “A stochastic analysis of long span structures subjected to spatially varying ground motions including the site-response effect”, Engineering Structures, 25, 2003: 1301-1310.
23. Tubino, F. Carassale, L. & S. Giovanni “Seismic response of multi-supported structures by proper orthogonal decomposition”, Earthquake Engineering and Structural Dynamics, Vol. 32, 2003: 1639-1654.
24. Zanardo, G. Hao, H, & C. Modena “Seismic response of multi-span simply supported bridges to a spatially varying earthquake ground motion”, Earthquake Engineering and Structural Dynamics, Vol. 31, 2002: 1325-1345.